Effects of Compact Radial-Vaned Air Separators on Stalling Characteristics of an Axial-Flow Fan

Nobuyuki Yamaguchi

Masayuki Ogata

Meisei University,
2-1-1 Hodokubo,
Hino-shi,
Tokyo 191-8506, Japan

Yohei Kato

Japan Filter Technology, Ltd.,
I-1-1 Aza Sugise,
Tsuhata-machi, Kawakita-gun,
Ishikawa Prefecture 929-0454, Japan

The stall-prevention effect of air separators incorporating radial vanes in place of the existing axial vanes was investigated on a low-speed, single-stage, lightly loaded axial-flow fan for effective and compact air separators of a simplified structure. From the survey, paying attention to several geometrical dimensions of the device, the following conclusions are obtained: (1) Simplified radial vanes made of flat plates could show strong stall-prevention effect comparable to those of the curved-vane type one. The most favorable ones showed no stall up to the fan shut-off conditions. (2) Radial heights of the recirculation passage within the air separator showed significant influences on the stall improvement. It should be larger than some critical size experimentally given in the study. (3) The axial length of the device should be larger than some critical size given experimentally in the study. Too much reduced axial length could give rise to an abrupt loss in the effect. (4) The optimum axial locations of the rotor-tip blade leading edge within the device inlet opening were found to lie near the center of the width of the inlet opening from both aspects of stall improvement and fan efficiency. [DOI: 10.1115/1.3104613]

Keywords: fluid machinery, fluid mechanics, axial-flow fan, fan stalling, antistall device, air separator

1 Introduction

Improved performance efficiency of turbomachines, such as gas turbines, jet engines, compressors, and fans, is desired in the fields of electric power generation, prime movers, and industrial plants from the point of view of not only the economy of operation but also the problems of global climate changes and energy security. The authors, aiming to raise both working efficiencies and operational safety of axial-flow compressors and fans, have strived for the improvement of stall and surge characteristics of the machines.

To improve stall characteristics of axial-flow fans and compressor stages, a variety of devices have hitherto been attempted, such as casing treatment, suction bypass, blade separator, and air separator, by many researchers and institutes (for example, see Refs. [1,2]). Among them, the present authors have paid attention to the air separator, especially the radial-vaned air separator, which was proposed by one of the authors [3,4]. The preceding study [5] has made clear that the radial-vaned air separator, Type A, has a significantly favorable and stable effect on stall prevention. In addition to that, experimental data on effects of several parameters on the stall-prevention effects and on the optimum relative dimensions and locations of the air separators of Type A were obtained.

In this report, as a continuation of the preceding study [5], the results of the experimental study toward simplification and compact sizing of the radial-vaned air separators will be described. The results, together with the preceding ones [5], will form a body of useful information and guidelines for practical application of the devices.

Contributed by the Turbomachinery Division of ASME for publication in the JOURNAL OF TURBOMACHINERY. Manuscript received September 5, 2008; final manuscript received November 27, 2008; published online January 12, 2010. Review conducted by Aspi Wadia.

2 Axial Fan for Test

The experimental fan is a single stage one of axial inlet type consisted of a rotor and exit guide vanes. The fan casing near the rotor tip was modified for mounting an air separator device. Table 1 gives main numerical figures about the fan. Table 2 gives blade geometrical data as measured for the rotor blades at the tip and the root. Each rotor blade is made of a twisted metal plate formed in circular-arc sectional shapes of 2 mm thickness. The rotor-tip clearance is 2 mm in radius.

With respect to the fan performances, fan flow rates Q were evaluated from the pressure difference of a Venturi tube located downstream of the fan for test. Fan rotor static-pressure rise Δp_S was evaluated from a difference in static pressures at an upstream suction duct wall and at the casing wall immediately downstream of the rotor blades. Fan power input P from the electric power input to the fan motor (after the inverter). Fan efficiency includes motor efficiency. The fan speed was set at 2600 rpm. The fan working conditions were regulated by throttling the exit valve of the fan test ducting. The details of the test facility are given in Yamaguchi et al. [5]. Fan stalling was judged to occur at the zero-slope point of the fan rotor total-pressure coefficient.

For flow coefficient φ_t below 0.20 in the stalled zone of the solid wall condition, reversal of strong swirling flow up to the suction duct inlet was observed [5]. Since the swirling flow reversal affected the accuracy in measurement of the fan pressure rise, the solid wall condition characteristics for flow coefficient above 0.2 is employed here for a basis for comparison. The fan Reynolds number based on the blade chord length and the blade tip speed was around 4×10^5. The uncertainty in pressure measurements is evaluated to be 1.5% [5].

3 Air Separator Devices

The terms "air separator" and "solid wall" are abbreviated AS and SW, respectively, hereafter in this report. Figure 1 shows symbols of variables that are inevitable in the process of optimizing

Table 1 Numerical data about the experimental fan

Casing diameter D_t	394 mm
Tip diameter	390 mm
Hub diameter D_h	194 mm
Tip clearance	2 mm
Fan speed	2600 rpm
Nominal motor power	1.5 kW
Nominal fan pressure rise	0.20 kPa
Nominal fan flow rate	100 m^3/min

the AS geometry. S and C are the respective widths of the inlet opening and the exit opening of the AS device, b is the width of the inner ring, W is the height of the internal passage, g and h are distances, respectively, from the upstream edge and the downstream edge of the AS inlet opening to the leading edge of the rotor-tip blade section, H is the fan annulus height, and Za is the axial chord of the rotor blade at its tip. Prototypical values of the present experimental machine are as follows:

$$H = 100 \text{ mm} \quad \text{and} \quad Za = 35 \text{ mm}$$

$$W = 33 \text{ mm}, \quad C = 43 \text{ mm}, \quad S = 37.5 \text{ mm}, \quad b = 25 \text{ mm}$$

In the course of the investigation, various dimensions were changed and adjusted.

The AS devices studied here are Types A, B, C, and D and Types 10 and 5. Type A is the one studied in the preceding study [5]. Types B, C, and D and Types 10 and 5 are discussed in Secs. 5 and 6, respectively.

4 Nondimensional Parameters

Performance results are normalized with respect to the blade tip speed u_t,

$$\text{Flow coefficient} \quad \phi_t = V_a/u_t \tag{1}$$

Table 2 Conditions of the rotor blades as measured

	Tip	Root
Number of rotor blades	6	
Chord length l (mm)	115	130
Blade spacing t (mm)	190	117.5
Pitch-chord ratio t/l	1.65	0.90
Stagger angle ξ	71 deg	43 deg
Camber angle θ	31.7 deg	43.5 deg

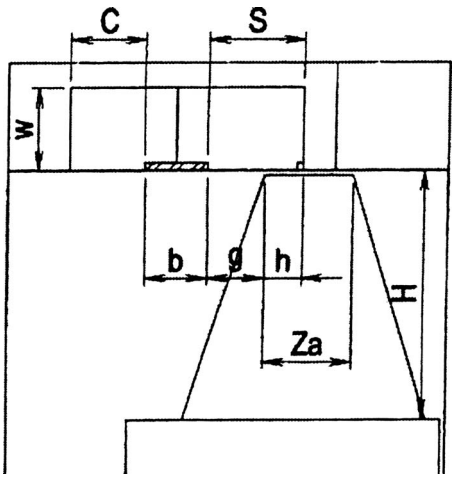

Fig. 1 Dimensions of the studied air separator and the fan

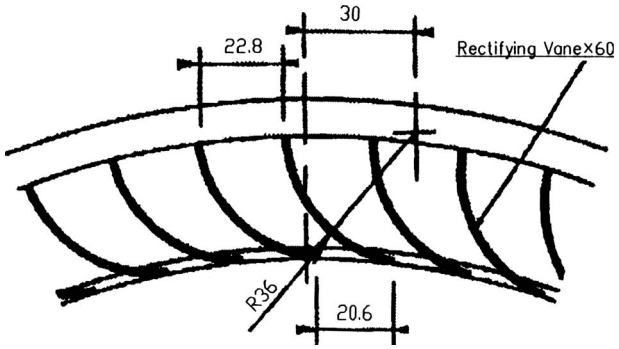

Fig. 2 Configuration of radial vanes for air separator Type A (W=33 mm)

$$\text{Rotor total-pressure coefficient} \quad \psi_t = \Delta p_T/\tfrac{1}{2}\rho u_t^2 \tag{2}$$

$$\text{Fan efficiency} \quad \eta_T = Q\Delta p_T/P \tag{3}$$

Here, Q is the fan flow rate (m^3/s), P is the motor power input (W), u_t is the fan rotor-tip speed (m/s), V_a is the annulus-average axial velocity (m/s), ρ is the air density (kg/m^3), Δp_S is the fan rotor static-pressure rise (Pa) between the suction duct wall pressure and the fan casing-wall pressure downstream of the rotor tip, and Δp_T is the fan rotor total-pressure rise (Pa),

$$V_a = Q/\left[\frac{\pi}{4}(D_t^2 - D_h^2)\right] \tag{4}$$

$$\Delta p_T = \Delta p_S + \tfrac{1}{2}\rho V_a^2[1 - (1 - \nu^2)^2] \tag{5}$$

Here, D_t and D_h, diameters of the fan casing and hub, respectively (m), and ν is the hub-to-tip radius ratio,

$$\nu = D_h/D_t \tag{6}$$

5 Trials of Simplified Radial-Vaned Air Separator

The preceding investigation [5] studied about the effects of AS Type A, about which the results are summarized as follows. Type A has radial vanes having a circular-arc sectional form, shown in Fig. 2, and numerical dimensions of W, C, S, and b listed in Sec. 3. The relative location of the leading edges of the rotor-tip blade section to the AS inlet opening that showed favorable results in the stall-prevention effect and the fan efficiency was for g/S of around 0.2–0.7. The characteristics of g/S of 0.4 is shown in Fig. 6 as AS-Aψ_t and AS-Aη_T. The effects of the relative location of the leading edges of the tip blade section on the stall flow coefficient ϕ_{tS} and the fan peak efficiency η_{TP} are shown in Fig. 9 as AS-Aϕ_{tS} and AS-Aη_{TP}.

In the continuation of the study [5], the authors have wished to make the AS devices simpler and more compact for easier practical applications. So, as the next stage, the following three types of simplified radial-vaned AS devices were tried. The sectional shapes of the radial vanes are changed to straight-plate ones in place of the circular-arc shape of Type A.

- Type B (Fig. 3): Radial vanes are simplified to inclined straight plates. The setting angle is 15 deg. W=33 mm.
- Type C (Fig. 4): Radial vanes are simplified to inclined straight plates. The setting angle is 45 deg. W=33 mm.
- Type D (Fig. 5): Radial vanes are simplified to inclined straight plates. The setting angle is 45 deg. W=11 mm, a third of those of Types A, B, and C.

Their axial dimensions C, S, and b are the same as those of Type A listed in Sec. 3. The relative radial heights of the AS passages are as follows:

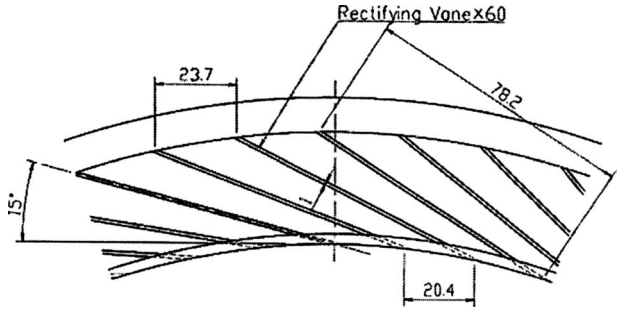

Fig. 3 Configuration of radial vanes for air separator Type B (*W*=33 mm)

$$W/H = 0.33(\text{Types A,B,C}), 0.11(\text{Type D})$$

$$W/Za = 0.94(\text{Types A,B,C}), 0.31(\text{Type D})$$

Figures 6 compares the performances effected by AS devices Types A, B, C, and D and the SW condition. Respective conditions are expressed as AS-A, AS-B, AS-C, AS-D, and SW in the figure. The relative locations of the leading edges of the rotor-tip blade sections to the AS inlet opening were kept the same as the optimum one for Type A, i.e., $g/S=0.4$ [5].

Both Types A and C eliminate the stall region over the entire flow coefficient. Type C shows a higher pressure coefficient at the shut-off condition. Types B and D prevent stalling over a very wide flow range but show a peak pressure coefficient around ϕ_t of 0.05 immediately before the shut-off condition, yielding a narrow positive-slope region.

With respect to the fan efficiency, all four AS devices show no steep drops in efficiency in the SW stalling zone. Type A keeps favorable efficiency comparable with the SW one in the SW sound condition and shows better level in the SW stalled zone. Types B and C show similar efficiency behaviors, in which the efficiency is lower by 1–2% than the SW one and is close to that of Type A in the SW stalled region. Type D shows an efficiency curve lower by 2–3% than those of SW and AS Type A over the whole flow range.

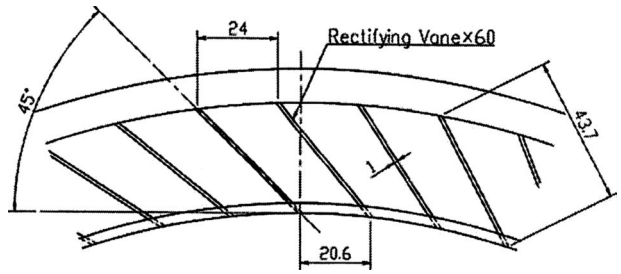

Fig. 4 Configuration of radial vanes for air separator Type C (*W*=33 mm)

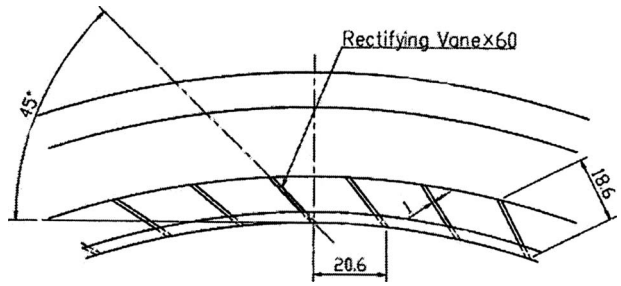

Fig. 5 Configuration of radial vanes for air separator Type D (*W*=11 mm)

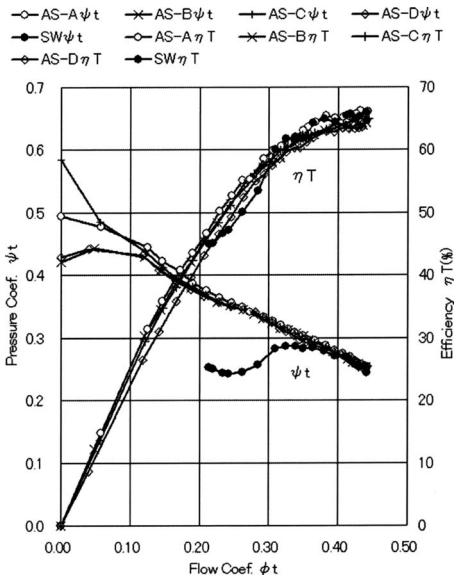

Fig. 6 Comparison of the effects of air separators of Types A–D together with the solid wall conditions on the fan characteristics

The following are summarized from the above observation.

(1) AS Type A is the best of the four from both viewpoints of stall prevention and fan efficiency level.
(2) The simplified configurations of the radial vanes are able to provide a large stall-prevention effect. However, some drops in the fan efficiency appear accompanied. The fan efficiency levels of Types B and C are comparable. Type C, which has a setting angle of 45 deg relative to the circumference, appears advantageous in suppressing stalling down to the shut-off condition.
(3) From the results on Type D, a reduction in the radial height of the AS passage is possible but tends to accompany some drops in the fan efficiency.

Related to the above item (2), the higher effectiveness in stall prevention up to the shut-off condition achieved by Type C compared with Type B could be explained very tentatively as follows. According to Tanaka and Murata [6] on a fan applied with a blade separator device, the meridional flow in the stall-improved region contains a large-scale recirculation flow forming an annular vortex ring, encasing the rotor blade tips, and extending toward the upstream of the separator and the rotor blade row. The recirculation flow is stabilized by flowing through the separator passage; thus the fan flow condition might be stabilized as a whole. The AS situation here could be similar to the above blade-separator one. So, it is supposed, though tentatively, that the flow rate through the AS passage might be relatively large near the shut-off condition, where the fan flow rate itself appears very small; thus, the higher setting angle of the radial vanes of Type C would be advantageous to treat with the large recirculation flow rate.

6 Effect of Height Reduction of the Radial-Vaned Air Separator

In order to put the AS devices to practical use, it is necessary to reduce the size for easier embeddability into casing walls of fans and compressors. From the aspect, the following two AS devices were made on the basis of the above results and some experiences of the authors for survey on the stall-prevention effects.

(1) AS Type 10: The radial height of the internal passage *W* is 10 mm. The vane configuration is shown in Fig. 7. Each vane is made of two pieces of straight plates: a main

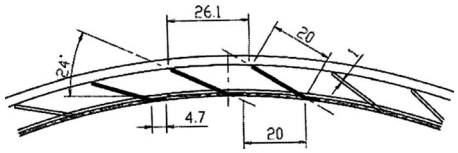

Fig. 7 Configuration of radial vanes for Type 10 air separator (*W*=10 mm)

straight plate of a length of 20 mm inclined at an angle of 24 deg to the casing circumference and a short front piece of a length of 4.7 mm attached circumferentially to the front edge of the main plate. Widths of the inlet opening and the exit one are $S=30$ mm and $C=45.5$ mm.

(2) AS Type 5: The radial height of the internal passage W is 5 mm. The vane configuration is shown in Fig. 8. Each vane is made of two pieces of straight plates: a main plate of a length of 12.4 mm inclined at an angle of 27.5 deg to the casing circumference and a front piece of a length of 4.8 mm attached circumferentially to the front edge of the main plate. Widths of the inlet opening and the exit one are $S=28$ mm and $C=43.5$ mm.

The short front plate attached to the main plate has two aims. The first is to approximate the vane configuration to a circular-arc one, as is seen for Type A. It could enhance the scooping action and will tend to reduce possible backflow reflected out of the AS passage into the fan main flow, which were often experienced in other types of AS devices. It has also an effect of increasing the row solidity. The second aim is, from a manufacturing point of view, to cut the whole row of the vanes out of only one long band of sheet metal or other materials. It could save the cost required for manufacturing or assembling the device out of many pieces.

6.1 Effects of Locations of the AS Devices Relative to the Rotor-Tip Blades. Effects of locations of the AS devices relative to the rotor-tip blade section on the stall prevention were surveyed by varying the dimensions g and h in Fig. 1, with the other dimensions kept the same as before. Figure 9 summarizes the behaviors of stall flow coefficients and peak efficiencies affected by the relative location g/S, including the results on AS Type A obtained in the preceding study [5]. In Fig. 9, symbol notes AS_A, AS_10, AS_5, and SW mean conditions of AS Type A, Type 10, Type 5, and SW, respectively. φ_{tS} and η_{TP} are the stalling flow coefficient and peak total efficiency, respectively. The behavior of the stall flow coefficients φ_{tS} in Fig. 9 shows that there exist favorable zones of relative location g/S for the maximum stall-prevention effect. For the smaller AS passage height W, the favorable zones are the narrower and the stall-prevention effects are the less. Type 5 shows a drastic reduction in both the zone width and its effectiveness in stall prevention in contrast to the very wide range of Type A that has achieved the complete unstalling down to the shut-off condition $\varphi_{tS}=0$. Nevertheless, Type 5 has a stalling flow coefficient of $\phi_{tS}=0.20$ in contrast to $\phi_{tS}=0.32$ for the SW condition.

As seen in Fig. 9, the stall-prevention effect disappears drastically at the upper limiting end of the optimum zone of g/S for all the AS types tested, which could be ascribed to a situation similar

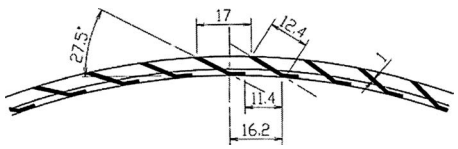

Fig. 8 Configuration of radial vanes for Type 5 air separator (*W*=5 mm)

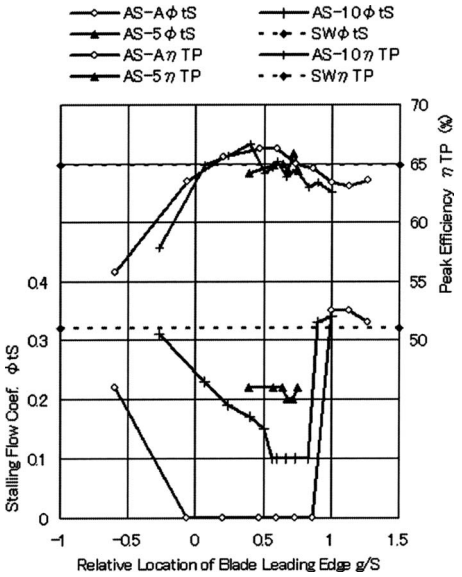

Fig. 9 Effects of relative locations of air separators Type A, Type 10, and Type 5 on the stalling flow coefficients and the peak efficiencies

to the deteriorated stall-prevention effect caused by retracted leading edges mentioned in the preceding study [5]. In the AS devices having a shorter passage height, the phenomenon appears even for the condition of the blade leading edges intruding into the axial width of the AS inlet opening. On the other hand, reduction in the effectiveness in the stall prevention toward the smaller g/S is seen rather gradually in Fig. 9, which could be related partly to the situation of the deteriorated stall-prevention effect caused by protruded leading edges described in the preceding study [5].

For the shorter-height AS devices, the peak-efficiency levels, whose accuracy is rather low and tentative, tend to be lower, and the favorable range becomes narrower compared with those of Type A condition.

6.2 Effects of the Widths of the Openings *S* and *C* of the AS Inlet and Exit. The effects of widths of the AS inlet and exit openings, S and C, were surveyed on the stall prevention, with the relative location g/S kept at respective optimum values selected from the above results. The employed values of g/S were 0.4 for Type A, 0.70 for Type 10, and 0.68 for Type 5. The inlet opening widths S were set by extending the width b of the AS inner ring by sticking adhesive tapes of a constant width on the radial-vane leading edges, and the exit openings C were set by inserting annular spacer rings with different thicknesses.

Figure 10 shows some typical behaviors of performance characteristics when the width C of the AS exit opening was changed with the width S of the inlet opening kept constant at 20 mm. In the symbol notes ($SxxCyy$) in Fig. 10, xx and yy mean the values of S and C in millimeters, respectively. It is seen that large stall-prevention effects are obtained for C larger than 10 mm. For the closed exit, i.e., $C=0$ mm, a certain degree of effect is seen to remain.

Figure 11 shows some typical behaviors of performance characteristics when the width S of the AS inlet opening was changed, with the width C of the exit opening kept constant at 20 mm. The symbol notes are expressed in quite the same manner as in Fig. 10. Stall-prevention effects by the AS devices are seen to be large but slightly changeable depending on the values of S and C.

6.3 Stall-Prevention Effect Affected by the Widths of the Openings of the AS Inlet and Exit. Since the stall-prevention effects are seen to vary depending on the combinations of the values of S and C, the variations in the effectiveness in functions

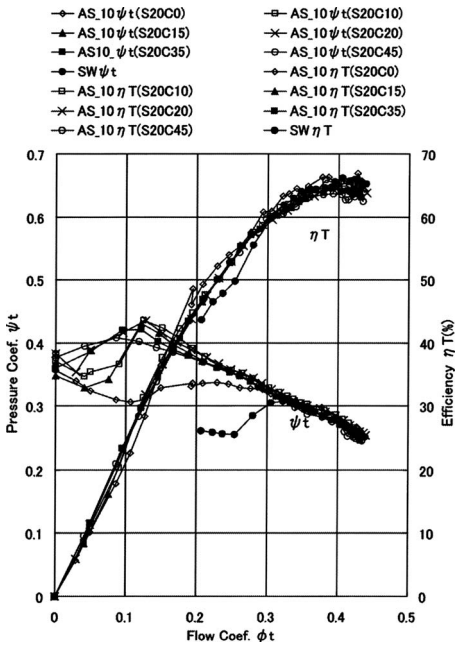

Fig. 10 Fan characteristics affected by the application of air separators Type 10 for $S=20$ mm and variable sizes of C

of S and C are summarized below. As a measure of stall-prevention effect, the following index B_s is employed:

$$B_S = [1 - (Q_S^*/Q_S)] \times 100(\%) \tag{7}$$

Here, fan flow rates at the stall point are expressed as Qs for the SW condition and Qs^* for the AS condition. For the case of no stall down to the shut-off condition, $Bs=100$, and in the case of no effect, $Bs=0$.

Figures 12 and 13 show contour maps for index B_S for AS devices Type 10 and Type 5, respectively, against of S and C. The iso-B_S lines are interpolated from data measured at "X" points on the maps.

The largest values of achieved B_S are 72.7 for Type 10, 39.4 for Type 5, and 100 for Type A [5], which are attained at the top-right points of the respective figures.

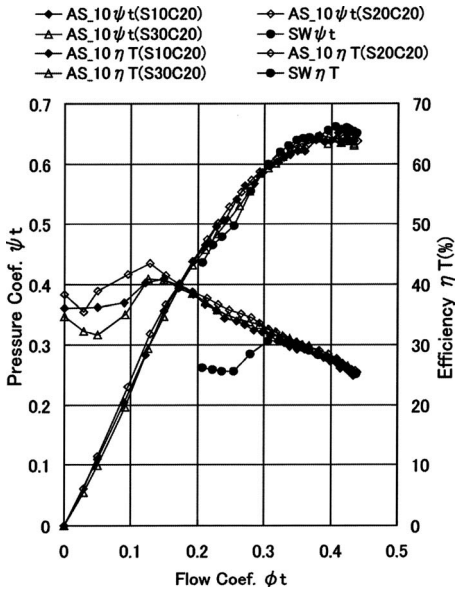

Fig. 11 Fan characteristics affected by the application of air separators Type 10 for $C=20$ mm and variable sizes of S

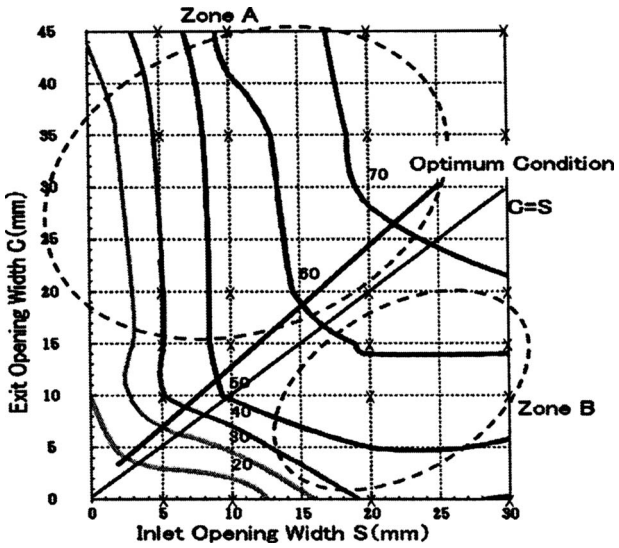

Fig. 12 Effects of opening widths of the inlet and the exit of air separator Type 10 on the stall improvement index Bs

Figures 12 and 13 show tendencies similar to those for Type A given in the preceding study [5]. There exist Zones A and B, where the iso-B_S lines are determined mostly by the inlet opening width S in the former and by the exit opening width C in the latter, respectively. Zone B for Type 5 in Fig. 13 is seen to be influenced by both S and C.

AS dimensions determined in such a manner as to minimize the additive value $(S+C)$ on each iso-Bs contour could minimize the axial size of the device for the Bs value. Such a condition is drawn as an optimum line, though very roughly, in Figs. 12 and 13. Line $C=S$, meaning the condition of equal widths of the inlet opening and the exit opening, is inserted for reference in the figures.

7 Summary and Considerations

7.1 Influence of Reduced Passage Height W. As seen in the decreasing order of the maximum Bs of AS devices Types A, 10, and 5, the reduction in the AS passage height W causes a signifi-

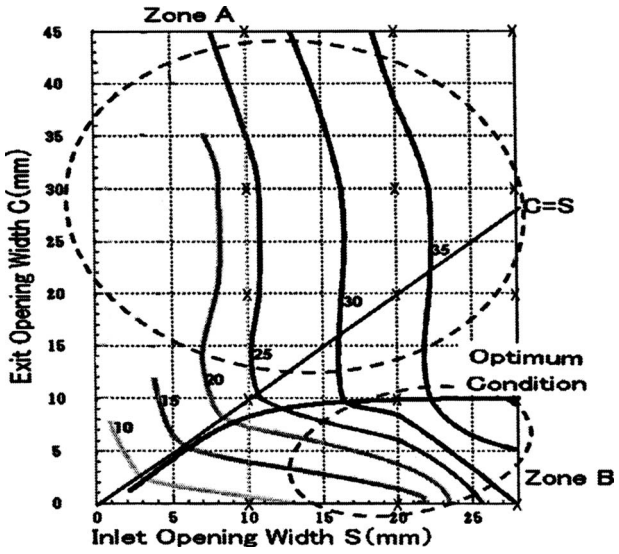

Fig. 13 Effects of opening widths of the inlet and the exit of air separator Type 5 on the stall improvement index Bs

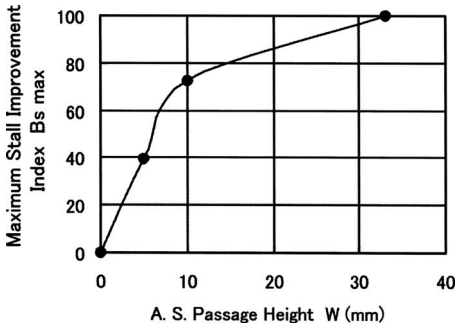

Fig. 14 Achieved maximum stall improvement indices *Bs* max for air separator passage height *W*

cant drop in the effectiveness of stall prevention. Figure 14 shows the tendency in the maximum *Bs* values affected by the passage height *W* of the respective AS devices, though including possibly some influences owing to the differences in the vane configurations. As seen in Fig. 14, devices smaller than Type 10 ($W=10$ mm) could have a steeply reduced *Bs* max value. As a measure, *W* larger than 10 mm for this particular fan is recommended. Or, in a relative form defined with the axial chord of the rotor-tip blade section *Za* as the reference length, W/Za larger than around 0.3 could be recommended.

The reduced effectiveness could be ascribed to the lowered capacity of the AS passage because of the insufficient passage height, i.e., reduction in the scooped flow rate in the inlet opening and incomplete discharge from the exit opening of the scooped flow.

7.2 Influence of the Axial Length of the AS Devices. Maximum values of stall improvement index *Bs* achievable by a given axial length of AS devices $(C+S)$ are plotted in Fig. 15, whose data are read from Figs. 12 and 13 in the present report and from Fig. 12 in the preceding report [5]. The right edge points of the curves are the respective maximum *Bs* max values shown in Fig. 14. It is seen that the highest magnitude of achievable *Bs* is determined mainly by the AS passage height *W* and that, with a decrease in the axial length $(C+S)$, the achievable *Bs* lowers. For further decrease in $(C+S)$, *Bs* tends toward 0. In order to obtain a level near *Bs* max, $(C+S)$ larger than roughly 45 mm for this particular fan or $(C+S)/Za$ larger than 1.3 in a relative form

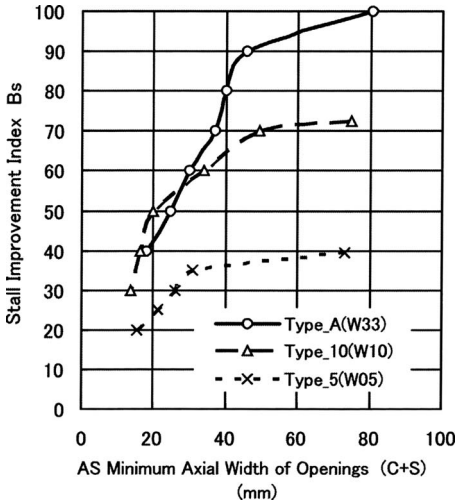

Fig. 15 Tendency of stall improvement indices *Bs* achievable for given axial widths of air separator openings *(C+S)*

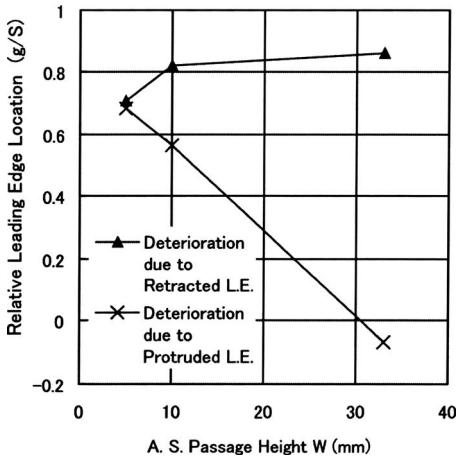

Fig. 16 Favorable range of *g/S* for stall improvement affected by the air separator passage height *W* for respective maximum widths of inlet and exit openings

would be necessary.

With respect to the respective lengths *S* and *C*, the optimum lines given in Figs. 12 and 13 in the present report and in Fig. 12 in the preceding report [5] could be referred to.

7.3 Favorable Relative Locations of the AS Devices. As shown in Fig. 9, with reducing AS passage height *W*, the favorable ranges of g/S become narrower, and at the same time the optimum location moves. The tendency is shown in Fig. 16 for the condition of the maximum widths of the AS openings. While the deterioration due to retracted leading edges is seen to occur roughly above g/S of around 0.8 common for the three types, the deterioration due to protruded leading edges and exposed blade tips are seen to occur earlier, with decreasing height of the devices. Accordingly, the optimum location moves from g/S of around 0.4 for Type A to around 0.7 for Types 10 and 5. For the smaller *W*, the deterioration due to protruded leading edges appears, with the leading edges located halfway in the axial width of the AS inlet opening, which suggests a more complicated situation than that supposed for Type A. As a possible situation in the relatively wide AS inlet openings, in addition to the above deterioration, a considerable part of the flow pushed into the inlet opening might have reflected back into free space in front of the blade tips in vain, only giving more disturbances to the main flow, thus reducing the probable stall-prevention effect.

7.4 Influence of Closed Exit Opening. Condition $C=0$ mm in Figs. 12 and 13 means a completely closed exit opening of the AS devices. For the condition, the rate of throughflow within the AS passage is zero. Even at this condition, a certain extent of the stall-prevention effect is seen to remain.

The authors suppose that, in the condition, the effect is helped by a mechanism similar to the casing treatment effect. The term "casing treatment" is abbreviated as CT hereafter. The stall-prevention effect by the CT (for example, see Ref. [7]) is considered as follows; while rotor-tip blade sections sweep the treated surface, the pressure-side high pressure of a blade pushes the air into the internal volume of the CT, and the pushed-in and compressed air blows back into the lower pressure region of the blade suction-side, blowing away the low-energy flow and making the tip environment cleaner.

As to AS Type 5 with the closed exit opening ($C=0$ mm), it is considered that the above phenomenon could have occurred and improved somewhat the stalling environment. In addition to that, as seen in Fig. 13, an increase in the width of the AS exit opening above *C* of around 10 mm does not cause further stall-prevention effects. It is conjectured that even when *C* is sufficiently large,

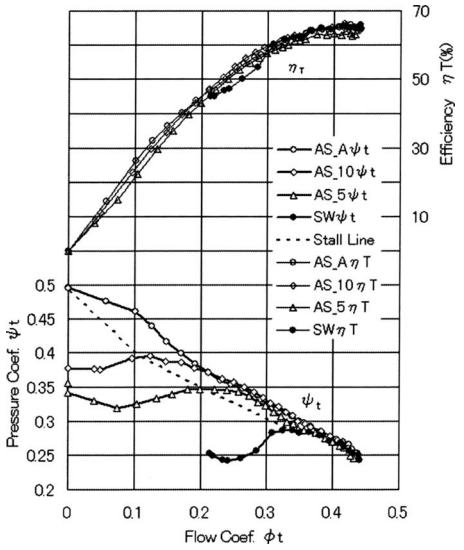

Fig. 17 Comparison of overall performances optimally improved by the applied air separators

Type 5 could not discharge all the scooped flow out of the exit opening, and a significant portion of the scooped flow might be reflected back at the inlet opening in a similar manner to the CT action.

In contrast to the above, the essential feature of the AS is to rectify all the scooped flow and discharge them out of the exit opening, which could be more effective if the conditions are well prepared. The situation of Type 10 seems to be halfway between those of Types A and 5.

7.5 Comparison of the Stall-Prevention Effects With Those of Casing Treatments. The order of magnitude of the stall-prevention index B_S in the CT application has been reported by Fujita and Takata [8] to be 20 in maximum and by Yamaguchi et al. [9] to be as large as 38 in maximum. The maximum *Bs* values of order of 40 obtained by Type 5 in this study are considered to be comparable to the highest possible level of those by CTs.

In consideration of the structural complexity of the AS devices compared with the simplicity of the CT structure, by far the more effective AS devices are desired for the practical application. For the purpose, an AS device with passage height W larger than 10 mm, which is equivalent to Type 10, is recommended for the particular fan condition. Or, in a relative form, W/Za greater than around 0.3 could be recommended as a measure.

7.6 Influence of the Thinner AS Devices on the Overall Performances. Figure 17 compares the best overall performances for the AS devices Types A, 10, and 5 and for the SW condition. It will be useful to predict the performance achieved by intermediate AS height conditions.

The stall points on the curves are seen lying on a dotted line nearly parallel to the pressure curve of Type A. It demonstrates the reduction in the stall-prevention effects with the reduction in the AS passage height. It suggests that the maximum recirculation flow rate allowable in the respective AS passages might have influences on the effectiveness.

According to Lee [10] on stall-improving effects by suction or injection through treated casing walls near the blade tips, the amount of the stall improvement depends greatly on the flow rate of the suction or injection. In the AS conditions, the recirculation flow rate will be determined in a self-balanced way, depending on several quantities, such as centrifuging forces of the flow, pressure losses within the AS passage, and wall pressure difference in the main flow between at the ASAS passage inlet and exit, many of which are intimately tied with the geometrical layout of the device and the relative arrangement of the blade tip and the AS device. In the smaller AS device, a sophisticated structure will be the key for success since the recirculation flow rate would naturally be smaller and the stall-prevention effects would be lower.

The efficiency curves show similar behaviors for the AS applied conditions. Peak efficiencies are the best for the conditions of SW and AS Type A. Type 5 shows some drop in the peak efficiency compared with the two. In the SW stalled region, all the AS applied conditions show improved efficiencies compared with the SW one.

8 Conclusion

The experimental study aimed to simplify the structure and reduce the sizes of radial-vaned air separators was conducted in the continuation of the preceding study [5]. By use of the AS devices equipped with simplified radial vanes made of inclined flat plates, the effects of the passage height W and the widths of the inlet opening and the exit opening, S and C, respectively, on the stall prevention were surveyed.

The following conclusions have been obtained, which are considered to be applicable to fans having conditions similar to the lightly loaded one tested here.

(1) AS devices equipped with radial vanes made of an inclined straight plate, when having a sufficiently large AS passage height (W), achieved favorable stall-prevention effects comparable to those of radial vanes having a circular-arc sectional shape (Type A [5]).
(2) AS passage height W exerted a significant influence on the stall-prevention effect. The height satisfying the condition $W/Za > 0.3$ is recommended if Za could be selected as an appropriate measure for the purpose. Below the level, drastic drops in the stall-prevention effects and the efficiencies could occur.
(3) Favorable relative locations g/S of the AS inlet opening relative to the leading edges of the rotor-tip blade section range roughly from 0.4 for large W to 0.7 for small W.
(4) A possible minimum axial length of the AS devices for a given stall-prevention index *Bs* could be determined as a condition for the minimum values of $(S+C)$ for the *Bs* value. As to the axial length, the value of $(S+C)/Za > 1.3$ is recommended.
(5) The stall-prevention effect by the smallest AS device, Type 5, with the exit opening closed ($C=0$), is comparable to the possible maximum effects achieved by casing treatments.
(6) Although AS devices are considered to have naturally a greater potential for stall prevention than that by CTs, the structures tend to be more complicated than those of CTs. Therefore, for practical use of the AS devices taking full advantages of the excellent potential, an AS size greater than Type 10 for the particular fan conditions or a relative passage height $W/Za > 0.3$ is recommended.

The authors consider that the above results have provided important basic data both from the practical point of view of developing more effective stall-prevention devices and from the phenomenological point of view of considering the mechanism of the AS effects. For highly loaded fans and compressor stages, further investigations are necessary, but the above results could be suggestive also in the study process.

Acknowledgment

The authors would like to express their deep thanks to the following graduate students of the Mechanical Department of Meisei University, Tokyo, Japan, who have devoted their efforts to the research: Mr. Mutsuhiro Ujihara, Mr. Kazuhiro Omichi, and Mr. Kazutaka Kumagai.

Nomenclature

b = axial length of the inner ring of the air separator (m)
Bs = index of improvement of stalling flow (%)
C = axial width of the exit opening of the air separator (m)
D_h = hub diameter of the fan (m)
D_t = casing-wall diameter of the fan (m)
g = distance between the leading edge of the rotor tip and the upstream edge of the inlet opening of the air separator (m)
h = distance between the leading edge of the rotor tip and the downstream edge of the inlet opening of the air separator (m)
H = annulus height of the fan (m)
l = chord length of the rotor bade (m)
P = power input to the driving motor (W)
Q = fan flow rate (m^3/s)
Q_S = stalling flow rate of the solid-wall fan flow rate (m^3/s)
Q_S^* = stalling flow rate of the fan with the air separator (m^3/s)
S = axial width of the inlet opening of the air separator (m)
t = spacing of neighboring blades (m)
u_t = peripheral speed of the rotor tip (m/s)
V_a = axial velocity (m/s)
W = height of the internal passage of the air separator (m)
Za = axial width of the rotor blade tip (m)
Δp_S = fan rotor static-pressure rise (Pa)
Δp_T = fan rotor total-pressure rise (Pa)
η_S = fan static efficiency
η_T = fan total efficiency
ρ = air density (kg/m^3)
θ = camber angle of the rotor blade (deg)
φ_t = fan flow coefficient
ψ_t = fan rotor total-pressure coefficient
ξ = stagger angle of the rotor blade (deg)

Indices

P = fan peak-efficiency point
t = normalized with reference to the rotor-tip speed
T = total pressure
S = static pressure or Stalling point
* = stalling point in the presence of the air separator

References

[1] Yamaguchi, N., 2005, "Stall and Surge of Axial Flow Compressors," Journal of Turbomachinery Society of Japan, **33**(8), pp. 490–502.
[2] Yamaguchi, N., 2005, "Stall Prevention by Means of Suction Rings and Casing Treatments, (1) Suction Rings and Casing Treatments," Journal of Turbomachinery Society of Japan, **33**(10), pp. 637–640.
[3] Yamaguchi, N., Takami, I., and Arimura, H., 1991, "Improvement of Air Separators of Axial Blowers," 250th Symposium of the Kansai Chapter of Japan Society of Mechanical Engineers, pp. 176–178.
[4] Yamaguchi, N., Owaki, T., Goto, M., Itaka, H., and Arimura, H., 1994, "Development of Mitsubishi General-Purpose Axial Fan (WIDEMAX Fan)," Tech. Rev.-Mitsubishi Heavy Ind., **31**(3), pp. 201–204.
[5] Yamaguchi, N., Ogata, M., and Kato, Y., 2008, "Improvement of Stalling Characteristics of an Axial Fan by Radial-Vaned Air Separator, Part I: Effects of Radial-Vaned Air Separators," Trans. Jpn. Soc. Mech. Eng., Ser. B, **074**(746), pp. 2163–2172.
[6] Tanaka, S., and Murata, S., 1975, "Post-Stall Characteristics and Rotating Stalls in an Axial Flow Fan, The Third Report: Stall Improvement Devices and Stalling Characteristics," Trans. Jpn. Soc. Mech. Eng., **41**(343), pp. 863–873.
[7] Takata, H., 1977, "Casing Treatment," The Fourth Seminar by Gas Turbine Society of Japan.
[8] Fujita, H., and Takata, H., 1981,"Study on the Effect of Casing Treatment Configuration in an Axial Flow Compressor," Jpn. Soc. Mech. Eng., preprint, No. 810-15, pp. 229–231.
[9] Yamaguchi, N., Otsukla, T., Higaki, K., Murakami, T., Goto, M., and Midori, M., 1983, "Development of Axial-Type Primary Air Fans for Coal-Fired Boilers: Development of Casing-Treated Adjustable Moving Blade Axial Fans," Tech. Rev.-Mitsubishi Heavy Ind., **20**(3), pp. 229–236.
[10] Lee, N. K. W., 1988, "Effects of Compressor Endwall Suction and Blowing on Stability Enhancement," MIT, GTL Report No. 192.